Stem Cell Reports
Article
OPEN ACCESS

Enhancer Analysis Unveils Genetic Interactions between TLX and SOX2 in Neural Stem Cells and In Vivo Reprogramming

Mohammed M. Islam,[1,4] Derek K. Smith,[1,2] Wenze Niu,[1,2] Sanhua Fang,[1,5] Nida Iqbal,[1] Guoqiang Sun,[3] Yanhong Shi,[3] and Chun-Li Zhang[1,2,*]
[1]Department of Molecular Biology
[2]Hamon Center for Regenerative Science and Medicine
University of Texas Southwestern Medical Center, 6000 Harry Hines Boulevard, Dallas, TX 75390, USA
[3]Department of Neurosciences, Cancer Center, Beckman Research Institute of City of Hope, 1500 E. Duarte Road, Duarte, CA 91010, USA
[4]Present address: College of Clinical Pharmacy, King Faisal University, Al-Ahsa 31982, Saudi Arabia
[5]Present address: Core Facilities of Zhejiang University Institute of Neuroscience, 866 Yuhangtang Road, Hangzhou 310058, China
*Correspondence: chun-li.zhang@utsouthwestern.edu
http://dx.doi.org/10.1016/j.stemcr.2015.09.015

SUMMARY

The orphan nuclear receptor TLX is a master regulator of postnatal neural stem cell (NSC) self-renewal and neurogenesis; however, it remains unclear how TLX expression is precisely regulated in these tissue-specific stem cells. Here, we show that a highly conserved *cis*-element within the *Tlx* locus functions to drive gene expression in NSCs. We demonstrate that the transcription factors SOX2 and MYT1 specifically interact with this genomic element to directly regulate *Tlx* enhancer activity in vivo. Knockdown experiments further reveal that SOX2 dominantly controls endogenous expression of TLX, whereas MYT1 only plays a modulatory role. Importantly, TLX is essential for SOX2-mediated in vivo reprogramming of astrocytes and itself is also sufficient to induce neurogenesis in the adult striatum. Together, these findings unveil functional genetic interactions among transcription factors that are critical to NSCs and in vivo cell reprogramming.

INTRODUCTION

Neural stem cells (NSCs) are self-renewing, multipotent progenitors with critical roles in the development of a functional nervous system and neuron differentiation (Alvarez-Buylla and Temple, 1998; McKay, 1997; Weiss and van der Kooy, 1998). Mounting evidence indicates that adult NSCs, which normally reside in the subgranular zone (SGZ) of the dentate gyrus (DG) and the subventricular zone (SVZ) of the lateral ventricle (LV), are essential for maintaining adult brain homeostasis (Gage, 2000; McKay, 1997; Rao, 1999). NSCs in these niches are critical to brain plasticity, but the molecular mechanisms governing these processes have yet to be elucidated.

The orphan nuclear receptor subfamily 2 group E member 1 (NR2E1), commonly known as TLX, has been identified as a fundamental regulator of adult NSCs and neurogenesis (Liu et al., 2008; Niu et al., 2011; Shi et al., 2004; Wang et al., 2013; Zhang et al., 2008). While TLX expression is observed in the forebrain and retina during early development, it becomes confined to NSCs of the DG and SVZ where neurogenesis continues into adulthood (Hollemann et al., 1998; Kitambi and Hauptmann, 2007; Monaghan et al., 1995). Even though no obvious defects are found in the brains of *Tlx* null mice during early development, mature mice exhibit limbic defects, retinopathies, reduced copulation, and progressively violent behavior (Islam and Zhang, 2015; Monaghan et al., 1997; Yu et al., 2000). The primary function of this key transcriptional regulator is to prevent the precocious differentiation of NSCs in the developing and adult brain (Li et al., 2008; Niu et al., 2011; Roy et al., 2004; Shi et al., 2004). TLX controls the expression of a broad network of genes to maintain NSC pools in an undifferentiated, self-renewing state (Niu et al., 2011; Shi et al., 2004, 2008; Zhang et al., 2008). TLX functions through the transcriptional suppression of target genes in association with other transcriptional corepressors like lysine-specific histone demethylase 1 (LSD1) (Sun et al., 2007, 2010, 2011; Yokoyama et al., 2008). Histone deacetylases (HDACs) are also recruited by TLX to target genes, which restrain transcription and, in turn, regulate NSC proliferation (Sun et al., 2007). While the essential roles of TLX in NSC self-renewal and differentiation have been well established, relatively little is known about the molecular mechanisms that govern the spatiotemporal expression of this critical factor in the developing and adult brain (Li et al., 2008; Roy et al., 2004; Shi et al., 2004, 2008).

To identify novel regulatory elements that will provide insight into this mechanism, we probed highly conserved sequences of the *Tlx* locus using in vitro screening and in vivo transgenic assays. Here, we have identified a single short DNA element bound by the transcription factors, sex determining region-box 2 (SOX2) and myelin transcription factor 1/neural zinc finger 2 (MYT1), which directly regulate *Tlx* expression in postnatal NSCs. We further unveiled

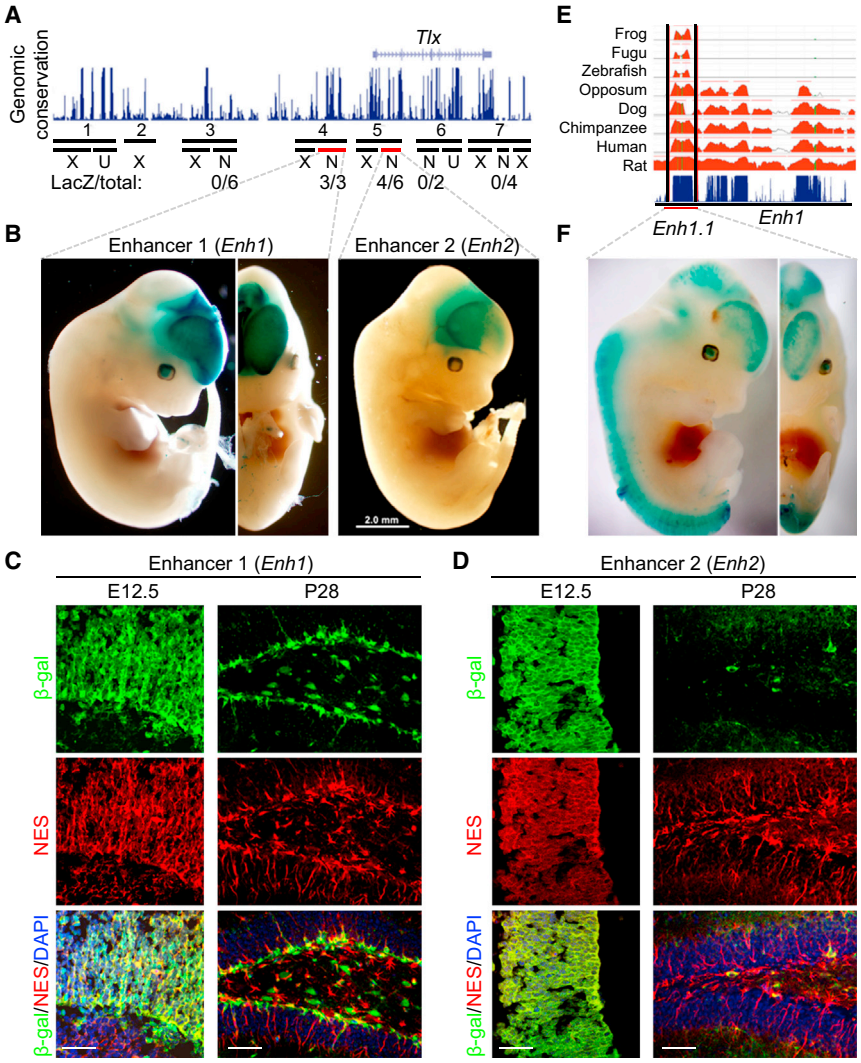

Figure 1. *Cis*-Regulatory Elements within the *Tlx* Locus

(A) Conservatory genomic elements and their role in controlling gene expression in neural stem cells (NSCs). The indicated elements were examined for driving gene expression in either cultured cells (X, not expressed; U, ubiquitous; N, NSCs) or transgenic mice (LacZ/total, $LacZ^{+}$ embryos over the total number of transgenic embryos).

(B) Brain-restricted reporter expression controlled by the identified two enhancers. Embryonic day (E) 12.5–13.5 embryos were stained for β-galactosidase activity.

(C) *Enh1* is active in both embryonic and postnatal stages. NSCs are marked with NES staining, while enhancer activity is indicated by staining for β-galactosidase (β-gal). E12.5, embryonic day 12.5; P28, postnatal day 28. The scale bar represents 50 μm.

(D) Enhancer activity of *Enh2* is developmentally regulated. The scale bar represents 50 μm.

(E) Genomic conservation of the indicated enhancer region.

(F) The highly conserved genomic sequence drives reporter expression (blue signal) in the developing CNS.

See also Figure S1.

that TLX mediates SOX2-dependent in vivo reprogramming of astrocytes in the adult mouse brain.

RESULTS

Identification of NSC-Specific Enhancers within the *Tlx* Locus

A cross-species comparison of genomic DNA sequences revealed multiple highly conserved regions within the *Tlx* locus (Figure 1A). To examine whether any of these conserved elements promote *Tlx* expression, we screened seven conserved DNA regions in cultured adult NSCs by linking the indicated genomic sequences to a β-galactosidase (β-gal) reporter. This systematic in vitro analysis revealed that five of these seven conserved regions were sufficient to drive β-gal reporter expression in NSCs, but not in other non-NSC lines, such as NIH 3T3, COS7, or HELA (Figure S1; data not shown). Next, a conventional in vivo transgenic analysis showed that only two of these regions, region 4 and region 5, were sufficient to drive reporter expression in the embryonic day (E) 12.5–13.5 forebrain in a pattern that resembles endogenous *Tlx* (Figures 1A and 1B) (Zhang et al., 2006). The first putative enhancer region (*Enh1*) we identified was a 3.3-kb fragment located 8 kb upstream of the *Tlx* transcription start site within region 4 (Figure 1A). The second putative enhancer region (*Enh2*) was a 4.2-kb fragment located within the first *Tlx* intron, a subsection of region 5 (Figure 1A). Both of these putative enhancers were capable of driving reporter expression in the developing forebrain and retina (Figure 1B). When analyzed at postnatal day (P) 28, signal intensity for the β-gal reporter remained robust for *Enh1* but tapered for *Enh2*. Further, *Enh2*-driven β-gal expression was dramatically reduced in adult neurogenic regions as compared to the *Enh1*-driven reporter (Figures 1C and

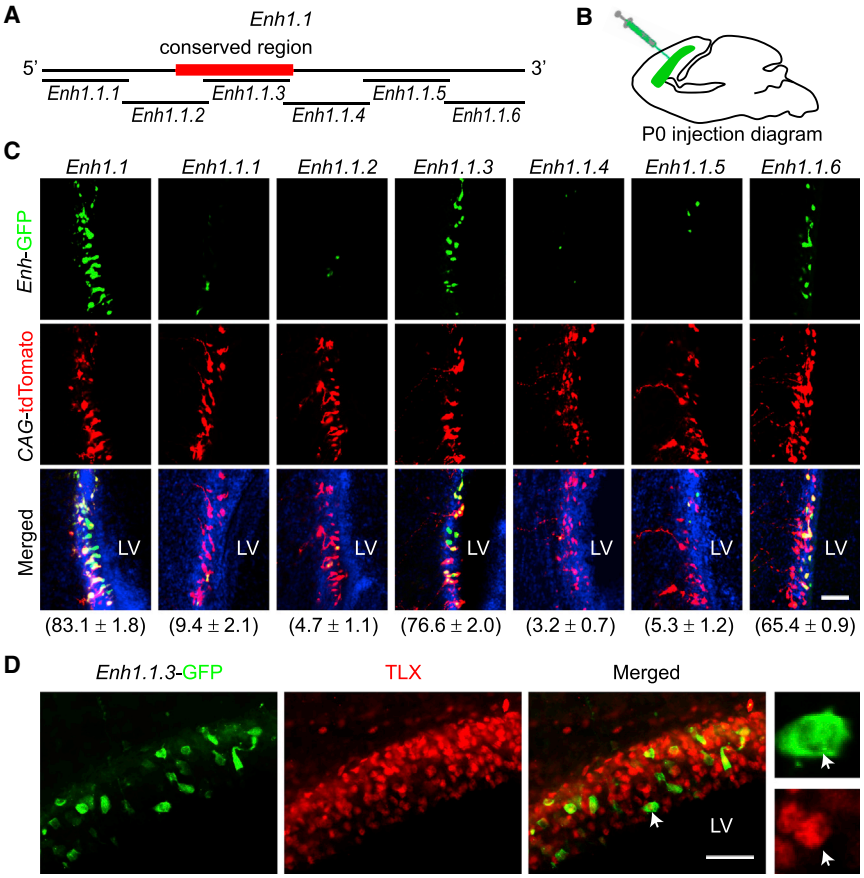

Figure 2. Core Sequences Controlling Gene Expression in TLX$^+$ Cells

(A) Relative sequence locations within the indicated *Tlx* enhancer.

(B) Analyzing enhancer activity through in vivo electroporation of P0 mouse brains.

(C) Representative fluorescence images showing transcriptional activity of the indicated genomic sequences. tdTomato under the constitutively active CAG promoter was used as an internal control for electroporation. The ratios of GFP$^+$ cells over tdTomato$^+$ cells are indicated in the parentheses (n = 3 mice; mean ± SEM). LV, lateral ventricle. The scale bar represents 50 μm.

(D) Immunohistochemistry showing enhancer activity in TLX$^+$ NSCs. Higher magnification views of the arrow-indicated cells are also shown. The scale bar represents 50 μm.

See also Table S1.

1D). Therefore, we opted to narrow the focus of our investigations to the enhancer activity of *Enh1*.

A second screen of smaller *Enh1*-derived DNA fragments uncovered a 582-nt region (*Enh1.1*) sufficient to drive reporter expression in cultured adult NSCs and transgenic E13.5 embryos (Figures 1E and 1F). Interestingly, *Enh1.1*-driven reporter expression is robustly detected throughout the developing CNS, indicating that neighboring elements of the full-length *Enh1* region act to restrict *Tlx* expression to the forebrain and retina during early development.

Enh1.1.3 Enhancer Is Active in TLX$^+$ NSCs

To define the minimal functional region of *Enh1* sufficient to drive *Tlx* expression, *Enh1.1* was subdivided into six roughly 120-bp overlapping fragments and then cloned into a GFP reporter vector (Figure 2A; Table S1). Each clone was co-electroporated with a control plasmid expressing tdTomato under the constitutively active *CAG* promoter into the forebrains of P0 mice (Figure 2B). GFP reporter expression was evaluated 5 days later (Figure 2C). Strong reporter expression was observed for the *Enh1.1* subregion *Enh1.1.3*, while *Enh1.1.6* induced moderate reporter signal (Figure 2C). Interestingly, the *Enh1.1.3* element falls within a highly conserved region of the *Tlx* locus (Figure 2A).

To validate *Enh1.1.3* as a bona fide *Tlx* enhancer, we analyzed the spatial expression pattern of this DNA element in the SVZ using a GFP reporter. An *Enh1.1.3*-GFP construct was electroporated into the LV of the P0 mouse forebrain, and reporter expression was evaluated 5 days later. Greater than 91% of *Enh1.1.3*-GFP$^+$ cells co-labeled with TLX, while only 63% of control *CAG*-GFP transduced cells were TLX$^+$, indicating robust transcriptional activity of this enhancer in postnatal NSCs (Figure 2D).

Enh1.1.3 Activity Requires SOX2 Binding

We next aimed to identify potential *trans*-acting factor binding sites within the *Enh1.1.3* enhancer. We used MatInspector to computationally identify 24 transcription factor binding sites, then narrowed our focus to four of these factors based on known molecular functions and spatiotemporal expression patterns (Cartharius et al., 2005). We used site-directed mutagenesis to delete one or more binding sites for each of these transcription factors and generated five *Enh1.1.3* mutant GFP reporter constructs, SOX2-BS1, SOX2-BS2, SOX2-BS1+BS2, MYT1, and

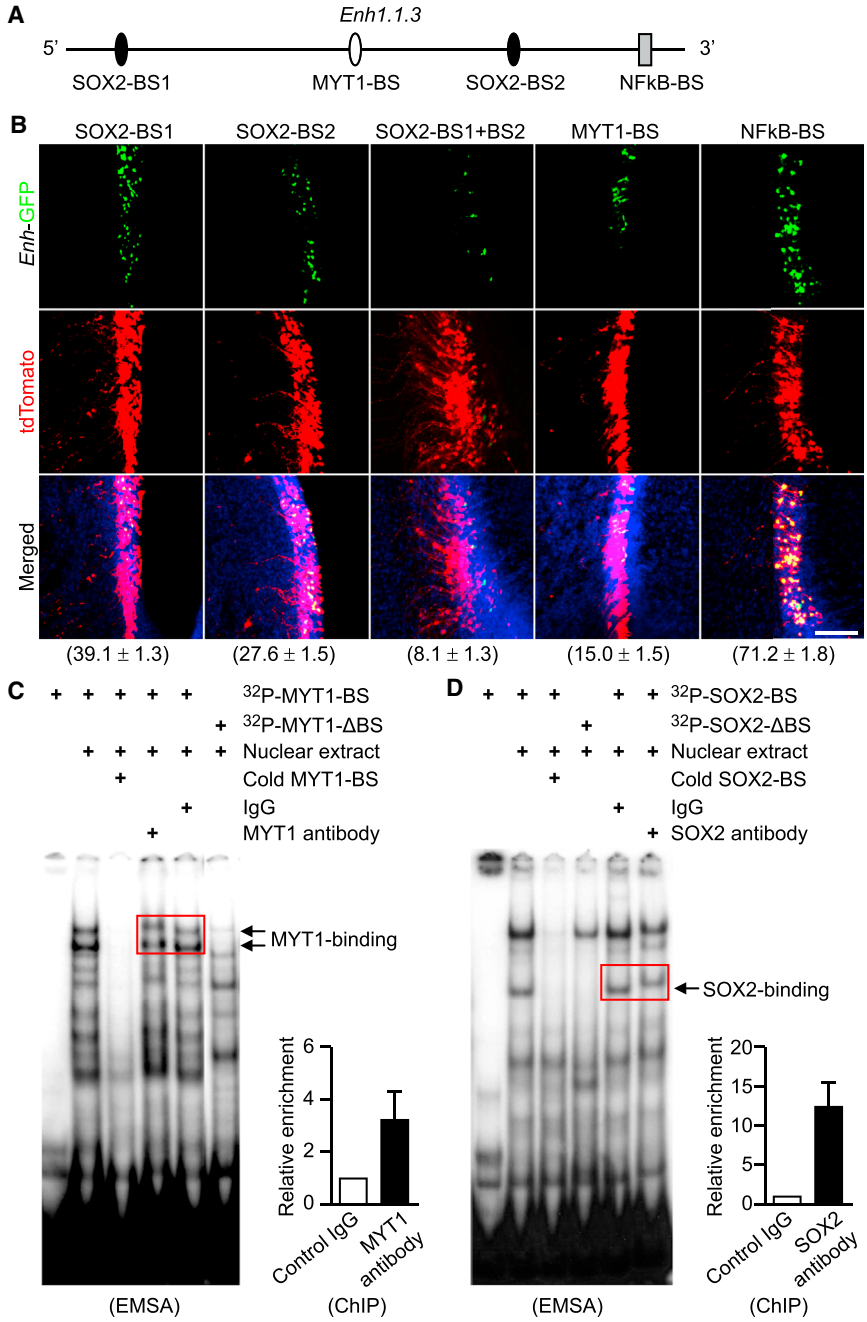

Figure 3. Transcription Factors Regulating *Tlx* Enhancer Activity

(A) A diagram showing locations of the consensus transcription factor binding sequences (BS).

(B) Diminished enhancer activity with mutations in the SOX2- or MYT1-binding sequences. Constitutively expressed tdTomato was used as an internal control for electroporation. The ratios of GFP^+ cells over $tdTomato^+$ cells are indicated in the parentheses (n = 3 mice; mean ± SEM). The scale bar represents 50 μm.

(C) MYT1 directly binds to the identified enhancer. Antibody-induced supershift in electrophoresis mobility shift assays (EMSA) is shown in the boxed region. Normal IgG was used as controls for EMSA and chromatin immunoprecipitation (ChIP) assays (mean ± SEM; n = 3 independent experiments for control IgG and MYT1 antibody).

(D) SOX2 directly binds to the identified enhancer. The boxed region shows antibody-induced supershift of the probe. Normal IgG was used as controls for EMSA and ChIP (mean ± SEM; n = 3 independent experiments for control IgG and SOX2 antibody).

See also Table S2.

NFκB (Figure 3A). Forebrain tissue electroporated with the NFκB-binding site-deleted construct showed no significant change in GFP reporter expression, whereas a moderate reduction of reporter activity was observed for constructs with mutations of SOX2-BS1 and SOX2-BS2, respectively (Figure 3B). Interestingly, the combined deletion of both SOX2-binding sites (SOX2-BS1+BS2) greatly diminishes GFP expression, indicating these sites are redundant but required for *Enh1.1.3 cis*-regulatory activity (Figure 3B). Unexpectedly, the deletion of these SOX2-binding sites from the full-length *Enh1.1 Tlx* regulatory element does not significantly alter enhancer activity (data not shown), suggesting additional redundancy among the five putative SOX2-binding sites within this larger enhancer region.

SOX2 and MYT1 Bind to *Enh1.1.3*

Similar to the deletion of SOX2-binding sites in *Enh1.1.3*, the deletion of a single MYT1-binding site moderately

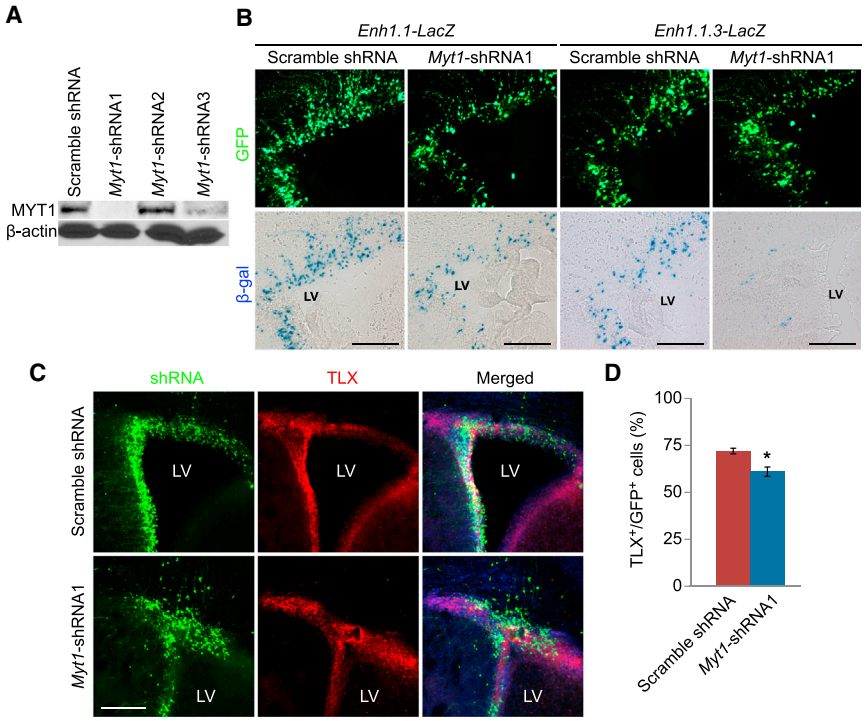

Figure 4. MYT1 Regulates *Tlx* Enhancer Activity

(A) A western blot analysis showing shRNA-mediated downregulation of MYT1. β-actin was used as a loading control.

(B) Knocking down endogenous MYT1 reduces transcriptional activity of the core enhancer (*Enh1.1.3*). shRNA-expressing cells are marked by GFP. The scale bar represents 100 μm.

(C) Immunohistochemistry showing TLX expression in cells with the indicated shRNA. The scale bar represents 100 μm.

(D) Downregulation of MYT1 modestly reduces the number of TLX-expressing cells (mean ± SEM; n = 3 mice for each shRNA; *p < 0.05 by Student's t test).

See also Table S3.

diminishes enhancer activity (Figure 3B). To confirm the sequence-specific binding of MYT1 to this predicted binding site, we performed an electrophoretic mobility shift assay (EMSA) (Figure 3C). A double-stranded DNA probe containing the MYT1-binding site within *Enh1.1.3* showed a distinct shift when incubated with NSC nuclear extracts, indicating a sequence-specific DNA-protein interaction (indicated by arrows in Figure 3C). Further, the addition of a MYT1-specific antibody induced a supershift not observed in the mock immunoglobulin G (IgG)-antibody-treated control (boxed region in Figure 3C). As expected, mutation of the MYT1-binding site in this probe resulted in the loss of specific protein binding (Figure 3C). These in vitro data strongly support MYT1 interaction with the *Enh1.1.3 Tlx* enhancer.

To confirm SOX2 sequence-specific binding to the *Enh1.1.3* enhancer element, we similarly performed EMSA with DNA probes specific to the *Enh1.1.3* SOX2-binding region. These complementary probes exhibited a specific shift when incubated with NSC nuclear extracts and were distinctly supershifted when incubated with SOX2-specific antibody (boxed region in Figure 3D). Moreover, mutation of the predicted SOX2-binding sites abolished this specific probe-SOX2 interaction (indicated by an arrow in Figure 3D). These results confirm the in vitro binding of SOX2 within the *Tlx cis*-element *Enh1.1.3*.

To validate the in vivo binding of these factors to *Enh1.1.3*, we performed chromatin immunoprecipitation (ChIP) assays using early postnatal mouse forebrains and antibodies specific to SOX2 or MYT1. qPCR analysis for the EMSA-identified MYT1-binding site showed a greater than 3-fold enrichment in MYT1 ChIP DNA over a mock IgG control (Figure 3C; ChIP). Similarly, SOX2 binding was confirmed with greater than 12-fold ChIP enrichment over IgG (Figure 3D; ChIP).

MYT1 Modulates *Tlx* Enhancer Activity

To determine the role for MYT1 binding within the *Enh1.1.3 Tlx* enhancer element, we analyzed the effects of short hairpin RNA (shRNA)-mediated *Myt1* knockdown on *E1.1.3* enhancer activity in vivo. A shRNA screen in HEK293 cells identified a highly efficient *Myt1*-targeting shRNA (*Myt1*-shRNA1; Figure 4A). Due to the lack of a suitable antibody for specific MYT1 immunohistochemical staining in the mouse forebrain, we co-electroporated *Enh1.1-LacZ* and *Enh1.1.3-LacZ* with *Myt1*-shRNA1 to determine whether MYT1 knockdown would significantly reduce reporter expression relative to a scrambled shRNA control. As shown in Figure 4B, MYT1 knockdown dramatically reduced the *Enh1.1.3*-driven β-gal expression but exhibited minimal effect on *Enh1.1*-driven reporter expression (Figure 4B). A moderate reduction in the number of TLX^+ cells was also

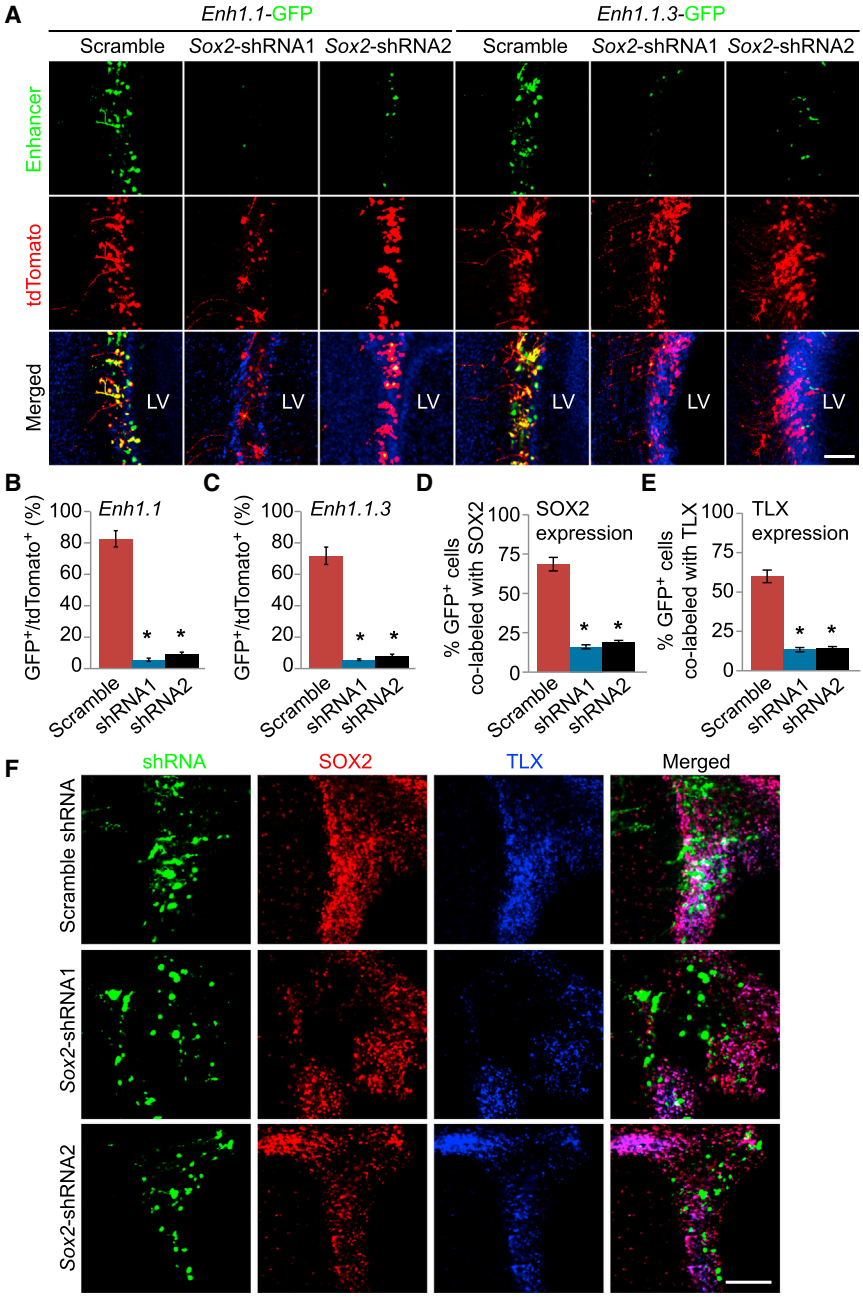

Figure 5. SOX2 Controls *Tlx* Enhancer Activity and Endogenous Expression

(A) Immunohistochemistry showing enhancer activity in cells with the indicated shRNA. The co-electroporated tdTomato was used as an internal control. The scale bar represents 50 μm.

(B) Downregulation of SOX2 greatly reduces *Enh1.1* activity (mean ± SEM; n = 3 mice for each shRNA; *p < 0.001 by Student's t test).

(C) Downregulation of SOX2 greatly reduces *Enh1.1.3* activity (mean ± SEM; n = 3 mice for each shRNA; *p < 0.001 by Student's t test).

(D) Quantification of SOX2 knockdown efficiency. shRNA-expressing cells are indicated by the co-electroporated GFP marker (mean ± SEM; n = 3 mice for each shRNA; *p < 0.01 by Student's t test).

(E) Downregulation of SOX2 dramatically reduces TLX expression (mean ± SEM; n = 3 mice for each shRNA; *p < 0.01 by Student's t test).

(F) Immunohistochemistry showing expression of the indicated markers. The scale bar represents 50 μm.

See also Table S3.

observed after *Myt1* knockdown (Figures 4C and 4D). Together, these results indicate that MYT1 controls the activity of a defined *Tlx* enhancer, but its activity is not a major driving force for the overall expression of endogenous *Tlx*.

SOX2 Controls *Tlx* Enhancer Activity and Endogenous Expression

To determine the role of SOX2 in the regulation of this enhancer, *Enh1.1-GFP* and *Enh1.1.3-GFP* were co-electroporated with two shRNAs targeting *Sox2* mRNA into the P0 mouse forebrain and analyzed 5 days later (Figure 5A). A scrambled shRNA sequence and the co-electroporated *CAG-tdTomato* were used as controls. *Sox2-shRNA1* and *Sox2-shRNA2* significantly reduced both *Enh1.1*- and *Enh1.1.3*-driven GFP expression (Figures 5A–5C). Downregulation of endogenous SOX2 expression by the two *Sox2* shRNAs was confirmed by immunohistochemical analysis of transfected cells that were labeled by a co-electroporated GFP reporter (Figures

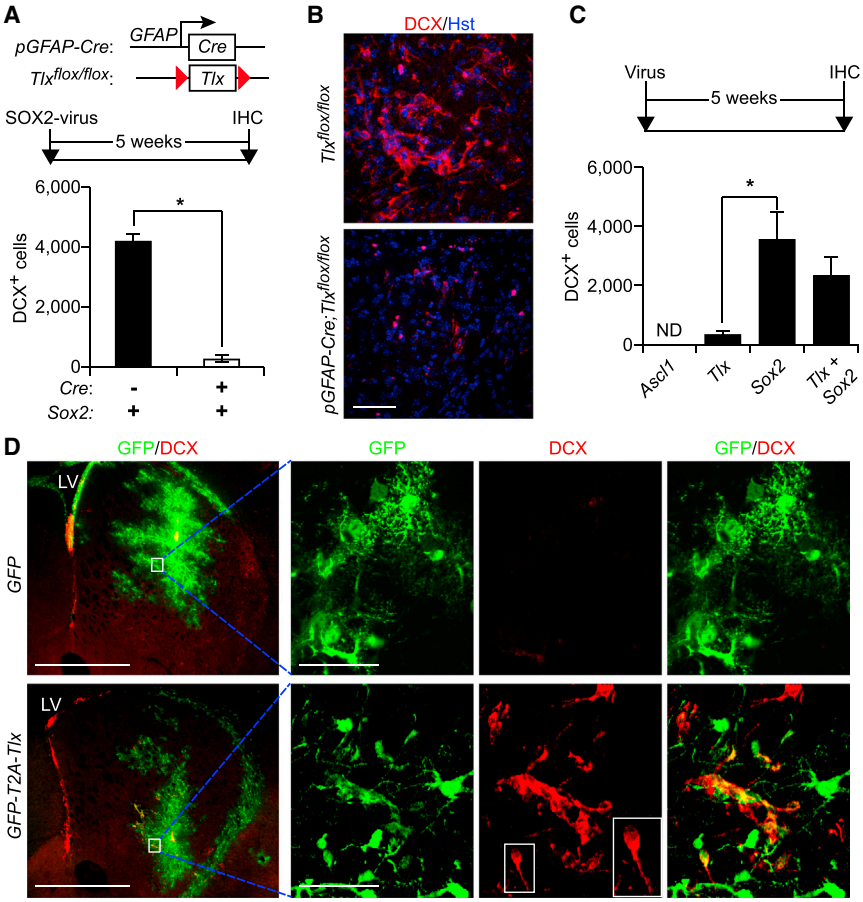

Figure 6. SOX2 Requires TLX to Induce Neurogenesis in the Adult Striatum

(A) TLX is required for SOX2-mediated in vivo reprogramming. *Tlx* was conditionally deleted in astrocytes of *pGFAP-Cre; Tlx*$^{flox/flox}$ mice. DCX$^+$ cells were quantified by immunohistochemistry (IHC) at 5 weeks post SOX2 virus injection in the adult striatum (mean ± SEM; n = 6 and 4 mice for *Cre*$^-$ and *Cre*$^+$ groups, respectively; *p < 0.001 by Student's t test).

(B) Representative confocal images showing SOX2-induced DCX$^+$ cells in the striatum of mice with the indicated genetic background. Hst, Hoechst 33342 dye. The scale bar represents 50 μm.

(C) Quantification of transcription factor-induced neuroblasts in the adult striatum. DCX$^+$ cells were determined by IHC at 5 weeks post virus injection in the adult mouse striatum (mean ± SEM; n = 5 mice for *Ascl1*, n = 5 mice for *Tlx*, n = 4 mice for *Sox2*, and n = 4 mice for *Tlx+Sox2*; ND, not detected; *p < 0.01 by Student's t test).

(D) Immunofluorescence showing TLX-induced DCX$^+$ neuroblasts in the adult mouse striatum. GFP alone was used as a control. An enlarged view of a DCX$^+$ cell in the boxed region is also shown. LV, lateral ventricle. The scale bar represents 1 mm (lower magnification views) and 50 μm (higher magnification views).

5D and 5F). Importantly, the expression of endogenous TLX is also dramatically reduced due to the downregulation of SOX2 in these cells (Figures 5E and 4F). This suggests a dominant role for SOX2 in the control of TLX expression.

TLX Is Required for SOX2-Mediated In Vivo Reprogramming

We and others recently showed that SOX2 can in vivo reprogram reactive glia into neural progenitors and neurons in the adult mouse brain and spinal cord (Heinrich et al., 2014; Niu et al., 2013, 2015; Su et al., 2014). As a direct downstream target of SOX2, we asked whether TLX plays a role during this in vivo reprogramming process. We conditionally deleted the *Tlx* gene in astrocytes of mutant mice harboring floxed *Tlx* alleles (*Tlx*$^{flox/flox}$) and a *Cre*-transgene controlled by the human *GFAP* promoter (*pGFAP-Cre*). SOX2-expressing lentivirus was injected into the striatum of adult control (*Tlx*$^{flox/flox}$) or *Tlx*-deleted (*pGFAP-Cre;Tlx*$^{flox/flox}$) mice. DCX$^+$ neuroblasts were quantified surrounding the virus-injected striatal regions at 5 weeks post virus injection (wpi). In contrast to control mice, the deletion of *Tlx* in astrocytes significantly decreased the detection of SOX2-induced DCX$^+$ cells in the adult striatum (Figures 6A and 6B).

Because of its essential role in maintaining adult neurogenesis (Liu et al., 2008; Niu et al., 2011; Shi et al., 2004; Zhang et al., 2008), we also examined whether TLX itself is sufficient to induce DCX$^+$ cells. Adult wild-type mice were stereotactically injected with lentivirus expressing transcription factors or a control GFP under the *GFAP* promoter. Immunohistochemistry was performed at 5 wpi. Very interestingly, DCX$^+$ neuroblasts were specifically observed in striatal regions with ectopic TLX but not ASCL1 or GFP (Figures 6C and 6D). Nevertheless, the total number of DCX$^+$ cells induced by TLX was significantly fewer than SOX2 alone, and their morphology was also very primitive, suggesting that additional factor(s) are required for robust in vivo reprogramming. Of note, the inclusion of TLX failed to enhance SOX2-induced adult neurogenesis (Figure 6C), which is consistent with our finding that TLX functions downstream of SOX2.

DISCUSSION

Although discovered more than two decades ago, the transcriptional regulation of *Tlx* in NSCs remains unclear (Yu et al., 1994). Numerous microRNAs such as let-7b and miR-137 have been identified as potential regulators of NSC proliferation, and a subset of these, miR-9 and let-7d, have been directly implicated in the regulation of TLX expression (Sun et al., 2011; Zhao et al., 2009, 2010). Similarly, interleukin-1 beta (IL-1β) has been shown to repress *Tlx* expression in neural precursor cells, differentiating newborn neurons, mature neurons, and astrocytes (Green and Nolan, 2012; Koo and Duman, 2008). However, the spatiotemporal mechanism that underlies *Tlx* transcription is undefined. In this study, we systematically examined the promoter and enhancer activity regulating *Tlx* expression in vivo and established genetic interactions between *Tlx* and two critical transcription factors, SOX2 and MYT1.

Comparative genomic analyses have proven to be a useful tool for identifying highly conserved regulatory elements that direct gene expression in a cell- or tissue-specific manner. Here, we identified two active regions, *Enh1* and *Enh2*, upstream of the *Tlx* transcription start site that are sufficient to drive the expression of a reporter gene at E13.5. Importantly, these two enhancers were not previously identified as SOX2-binding regions in cell culture (Shimozaki et al., 2012), which indicates the mechanisms regulating physiological *Tlx* expression might be significantly different from in vitro models. The systematic analysis of a transcriptional enhancer we termed *Enh1* led to the identification of *Enh1.1*, a 582-bp *cis*-regulatory region active in the developing forebrain, retina, and other regions of the CNS. We subdivided the sequence of this putative enhancer to identify the highly conserved 120-bp *cis*-element *Enh1.1.3*. This element is preferentially active in TLX^+ cells in the SVZ of LV and is sufficient to drive reporter gene expression. In contrast to NSCs, other populations of cells in the SVZ did not exhibit *Enh1.1.3* activity, which highlights the transcriptional specificity of this element. In addition, a second subregion of *Enh1*, *Enh1.1.6*, moderately activated reporter expression, potentially indicating that multiple redundant transcription factor binding sites exist within the *Tlx* enhancer.

Four potential transcription factor binding sites were identified and investigated by site-directed mutagenesis based on their known functions and expression patterns (Avilion et al., 2003; Bellefroid et al., 1996; Graham et al., 2003; Pevny and Nicolis, 2010; Shi et al., 2008; Shimozaki et al., 2012). The individual deletion of SOX2-binding sites only moderately affected *Enh1.1.3* activity; however, the deletion of both sites severely abolished reporter expression. This functional redundancy might explain why the deletion of these two binding sites did not affect the activity of *Enh1.1*, which contains at least five SOX2-binding motifs. The deletion of a ChIP-validated MYT1-binding site repressed *Enh1.1.3* activity, indicating the mechanism underlying *Tlx* expression is complex and involves multiple factors. These observations were validated by EMSA binding assays and in vivo ChIP assays. Further, *Sox2* knockdown dramatically reduced *Enh1.1* and *Enh1.1.3* activity and significantly reduced TLX expression in vivo. *Myt1* knockdown affected only *Enh1.1.3* activity and moderately repressed in vivo TLX expression. This suggests a specific MYT1-*Enh1.1.3* interaction that fine-tunes the expression of *Tlx* in NSCs. As a recently identified subunit of the lysine-specific demethylase 1 complex, a corepressor of *Tlx*, MYT1 might exert unique control over the onset of neurogenesis and neural differentiation in adult NSCs (Armstrong et al., 1995, 1997; Kim et al., 1997; Matsushita et al., 2014).

Collectively, these data demonstrate that SOX2 and MYT1 regulate the spatiotemporal expression of *Tlx* in NSCs during postnatal development. The ectopic expression of SOX2, a transcription factor with well-defined roles in stem cell pluripotency and transcriptional regulation (Avilion et al., 2003; Catena et al., 2004; Graham et al., 2003; Lorthongpanich et al., 2008; Masui et al., 2007; Pevny and Nicolis, 2010; Rossant, 2004; Sarkar and Hochedlinger, 2013; Shimozaki et al., 2012; Suh et al., 2007), was recently shown to reprogram reactive glia into neural progenitors and neurons in the adult mouse brain and spinal cord (Niu et al., 2013, 2015; Su et al., 2014). Our current data further demonstrate that SOX2-regulated *Tlx* expression is required for this in vivo reprogramming process. These findings provide new insights into molecular mechanisms that govern NSC behavior and fate reprogramming.

EXPERIMENTAL PROCEDURES

Animals

Wild-type C57BL/6 and ICR mice were obtained from The Jackson Laboratory and Harlan Laboratory, respectively. The generation of $Tlx^{flox/flox}$ mice was previously described (Zhang et al., 2008). The transgenic *pGFAP-Cre* mice were created by the laboratory of Albee Messing (Zhuo et al., 2001) and purchased from The Jackson laboratory (stock number 004600). All mice were housed under a 12-hr light-dark cycle with ad libitum access to food and water in a controlled animal facility. All experimental protocols were approved by the Institutional Animal Care and Use Committee at The University of Texas Southwestern Medical Center.

Bioinformatics

The UCSC genome browser was used to retrieve sequences and annotations for the mouse *Tlx* gene and its cross-species homologs. Transcription factor binding sites in *E1.1.3* were identified using the MatInspector application within the Genomatix Suite.

DNA Constructs and Site-Directed Mutagenesis

Assays for the activity of candidate *Tlx cis*-elements were performed using a human β-globin promoter plasmid carrying either a *LacZ* or *GFP* reporter. Evolutionarily conserved noncoding and coding subregions of the *Tlx* locus were PCR amplified and cloned to generate DNA constructs. Two constructs, *CAG-GFP* and *CAG-tdTomato*, were used as transfection controls. A plasmid carrying the full-length mouse *Myt1* cDNA was obtained from Addgene (plasmid 22713) and subcloned into a pCMX vector to generate a *Myt1* construct with an amino terminus HA-tag for overexpression in knockdown studies. A PCR-based site-directed mutagenesis method was used to generate mutant enhancer constructs. Briefly, mutations were introduced by PCR using a set of primers with either a deletion or point mutation in the targeted binding site and then validated by DNA sequencing.

In Vivo DNA Electroporation

Mouse P0 forebrain DNA electroporation was performed essentially as previously described (Boutin et al., 2008). Briefly, a 2-μl mixture of plasmid DNA and fast green FCF dye (4 μg/μl and 2 μg/μl final concentrations, respectively) was directly injected into the LVs of the P0 mouse forebrain using a glass micropipette. Five electric pulses (88 V, 50-ms duration, 950-ms intervals) were applied through the head with a CUY21 electroporator (Nepagene).

Immunohistochemistry

Mice were sacrificed, perfused with PBS, and then perfused by ice-cold 4% paraformaldehyde (PFA) in PBS. Brains were dissected and postfixed overnight with 4% PFA at 4°C followed by cryoprotection in a 30% sucrose solution overnight. Frozen brains were sectioned at 40 μm with a sliding microtome (Leica Microsystems). Free-floating sections were washed three times with PBS and blocked for 1 hr at room temperature (3% BSA and 0.2% Triton X-100 in PBS). The sections were immunostained overnight at 4°C with anti-SOX2 antibody (SC17320, goat, 1:500, Santa Cruz) diluted in blocking solution. After three rinses with wash buffer (0.2% Triton X-100 in PBS), the sections were incubated with Alexa-Fluor-594-conjugated secondary antibody (Jackson ImmunoResearch) in blocking solution for 2 hr at room temperature. Nuclei were stained with Hoechst 33342 (1 μg/ml, Sigma). Images were obtained on a Zeiss LSM510 confocal microscope. A Cell Counter software plugin for ImageJ was used to count cells. A representative image is shown from at least three similar images.

EMSA

Complementary single-stranded oligonucleotides were designed to mimic the Enh1.1.3 DNA sequence including consensus SOX2- and MYT1-binding sites (Sigma Aldrich). Complimentary oligonucleotides were annealed and labeled with ^{32}P-dCTP (2×10^5 counts per minute). Nuclear extract (5 μg) isolated from E14 mouse forebrain was incubated with ^{32}P-dCTP-labeled probes in binding buffer (10 mM HEPES [pH 7.8], 50 mM KCl, 1 mM EDTA, 10% glycerol, 1 mM DTT, and 50 μg/ml poly(dI:dC)) for 20 min at room temperature. Antibody-mediated supershift assays were incubated with 1 μg anti-MYT1 antibody (AB30997, rabbit, Abcam) or 1 μg anti-SOX2 antibody (AB5603, rabbit, Millipore) for an additional 15 min. The DNA-protein complexes were separated on 5% non-denaturing polyacrylamide gels and detected by autoradiography.

Western Blot Analysis

Harvested cells were treated with lysis buffer (50 mM Tris-HCl [pH 7.5], 150 mM NaCl, 1 mM EDTA, 0.5% sodium deoxycholate, 1% NP-40, and protease inhibitors [Roche]) for 30 min at 4°C. Protein samples were separated on 10% SDS-polyacrylamide gels, transferred to polyvinylidene difluoride membranes (Millipore), and blotted with corresponding primary and secondary antibodies for chemiluminescence detection (Amersham). The following primary antibodies were used: monoclonal anti-β-actin, clone ac-74 (A5316-100μL, mouse, 1:8,000, Sigma-Aldrich), and HA epitope (MMS-101P, mouse, 1:1,000, Covance).

ChIP and Quantitative Real-Time PCR

Approximately 0.1 g of P5 mouse forebrain was excised from surrounding neural tissue and crosslinked with 1% methanol-free formaldehyde for 10 min at room temperature. The reaction was quenched with glycine (0.125 M final concentration) and the tissue washed twice with ice-cold PBS. Tissue was suspended in 5 ml lysis buffer (100 mM HEPES [pH 8.0], 85 mM KCl, 1% IGEPAL CA-630, and EDTA-free complete protease inhibitor [Roche]) for 20 min on ice then homogenized by douncing. Nuclei were pelleted, resuspended in 275 μl shearing buffer (50 mM HEPES [pH 8.0], 10 mM EDTA [pH 8.0], 1% SDS, EDTA-free complete protease inhibitor), and chromatin sheared for 45 min at 4°C using a Bioruptor (Diagenode) until DNA fragments were 200–600 bp. Sheared chromatin (50 μg) was diluted 10-fold in immunoprecipitation buffer (50 mM HEPES (pH 8.0], 20 mM NaCl, 1 mM EDTA [pH 8.0], 0.1% Triton X-100, EDTA-free complete protease inhibitor) and immunoprecipitated with anti-SOX2 (AB5603, rabbit, 5 μg, Millipore), anti-MYT1 (HPA006303, rabbit, 5 μg, Sigma), or anti-IgG (PP64, rabbit, 5 μg, Millipore) at 4°C for 14 hr. Protein G magnetic Dynabeads (100 μl, Life Technologies) were used to isolate immunoprecipitated chromatin at 4°C for 2 hr. The immunoprecipitated fraction was washed twice with immunoprecipitation buffer, twice with wash buffer (100 mM Tris-HCl [pH 9.0], 500 mM LiCl, 1% IGEPAL CA-630, 1% deoxycholic acid, and EDTA-free complete protease inhibitor) and one time with high salt wash buffer (wash buffer containing 150 mM NaCl). Chromatin was eluted in 100 μl elution buffer (1% SDS, 50 mM sodium bicarbonate) at 25°C for 30 min with shaking. Eluted chromatin was treated with 1 μl RNase A (10 μg/μl) and 2 μl Proteinase K (40 μg/μl) at 37°C for 1 hr, and then then crosslinking was reversed with NaCl (333 mM final concentration) at 67°C for 14 hr. Immunoprecipitated DNA was purified using the QIAquick PCR Purification Kit (QIAGEN) according to the manufacturer's specifications. Quantitative real-time PCR was performed to determine the fold-enrichment of SOX2 and MYT1 immunoprecitated DNA relative to background in IgG-treated samples (primer sequences listed in Table S2).

shRNA-Mediated SOX2 and MYT1 Knockdown

Mouse P0 forebrains were transfected with *Sox2*- and *Myt1*-specific shRNAs or scrambled control (OriGene). All shRNAs were

subcloned into the Superscript-*GFP* vector (shRNA sequences listed in Table S3).

Virus Generation and Stereotactic Injections

The lentiviral vectors *GFAP-GFP*, *GFAP-Sox2*, *GFAP-GFP-T2A-Tlx*, and *GFAP-Ascl1* were generated as previously described (Niu et al., 2013). Under the guidance of a stereotactic apparatus (Stoelting), a total volume of 2 μl purified virus, each with a titer of 0.5–1 × 10^9 colony-forming units per 1 ml, was injected into the striatum of adult mice. The injection coordinates follow: +1.0 mm (anterior-posterior), ±2 mm (medial-lateral), and −3.0 mm (dorsal-ventral from the skull).

Statistical Analysis

Data are presented as mean ± SEM. Statistical analysis was performed by a two-tailed unpaired Student's t test. Any p value < 0.05 was considered significant.

SUPPLEMENTAL INFORMATION

Supplemental Information includes one figure and three tables and can be found with this article online at http://dx.doi.org/10.1016/j.stemcr.2015.09.015.

AUTHOR CONTRIBUTIONS

M.M.I. and C.-L.Z. conceived and designed the experiments. M.M.I., D.K.S., W.N., S.F., and N.I. performed the experiments. G.S. and Y.S. provided critical reagents and comments. M.M.I., D.K.S., and C.-L.Z. prepared the manuscript.

ACKNOWLEDGMENTS

We thank Hiro Tanda for assistance with preliminary experiments and data collection, as well as other members of the C.-L.Z. laboratory for discussions and technical support. We are grateful to Jane E. Johnson (The University of Texas Southwestern Medical Center) and Li Cai (Rutgers University) for generously providing β-GP-*LacZ* and β-GP-*GFP* plasmids, respectively. C-L.Z. is a W.W. Caruth, Jr. Scholar in Biomedical Research. This work was supported by the Welch Foundation Award (I-1724), the Ellison Medical Foundation Award (AG-NS-0753-11), Texas Institute for Brain Injury and Repair, the Decherd Foundation, and NIH grants (R01NS070981, R01NS088095, R21NS093502, and DP2OD006484 to C.-L.Z.).

Received: May 28, 2015
Revised: September 16, 2015
Accepted: September 17, 2015
Published: October 22, 2015

REFERENCES

Alvarez-Buylla, A., and Temple, S. (1998). Stem cells in the developing and adult nervous system. J. Neurobiol. *36*, 105–110.

Armstrong, R.C., Kim, J.G., and Hudson, L.D. (1995). Expression of myelin transcription factor I (MyTI), a "zinc-finger" DNA-binding protein, in developing oligodendrocytes. Glia *14*, 303–321.

Armstrong, R.C., Migneault, A., Shegog, M.L., Kim, J.G., Hudson, L.D., and Hessler, R.B. (1997). High-grade human brain tumors exhibit increased expression of myelin transcription factor 1 (MYT1), a zinc finger DNA-binding protein. J. Neuropathol. Exp. Neurol. *56*, 772–781.

Avilion, A.A., Nicolis, S.K., Pevny, L.H., Perez, L., Vivian, N., and Lovell-Badge, R. (2003). Multipotent cell lineages in early mouse development depend on SOX2 function. Genes Dev. *17*, 126–140.

Bellefroid, E.J., Bourguignon, C., Hollemann, T., Ma, Q., Anderson, D.J., Kintner, C., and Pieler, T. (1996). X-MyT1, a Xenopus C2HC-type zinc finger protein with a regulatory function in neuronal differentiation. Cell *87*, 1191–1202.

Boutin, C., Diestel, S., Desoeuvre, A., Tiveron, M.C., and Cremer, H. (2008). Efficient in vivo electroporation of the postnatal rodent forebrain. PLoS ONE *3*, e1883.

Cartharius, K., Frech, K., Grote, K., Klocke, B., Haltmeier, M., Klingenhoff, A., Frisch, M., Bayerlein, M., and Werner, T. (2005). MatInspector and beyond: promoter analysis based on transcription factor binding sites. Bioinformatics *21*, 2933–2942.

Catena, R., Tiveron, C., Ronchi, A., Porta, S., Ferri, A., Tatangelo, L., Cavallaro, M., Favaro, R., Ottolenghi, S., Reinbold, R., et al. (2004). Conserved POU binding DNA sites in the Sox2 upstream enhancer regulate gene expression in embryonic and neural stem cells. J. Biol. Chem. *279*, 41846–41857.

Gage, F.H. (2000). Mammalian neural stem cells. Science *287*, 1433–1438.

Graham, V., Khudyakov, J., Ellis, P., and Pevny, L. (2003). SOX2 functions to maintain neural progenitor identity. Neuron *39*, 749–765.

Green, H.F., and Nolan, Y.M. (2012). Unlocking mechanisms in interleukin-1β-induced changes in hippocampal neurogenesis–a role for GSK-3β and TLX. Transl. Psychiatry *2*, e194.

Heinrich, C., Bergami, M., Gascón, S., Lepier, A., Viganò, F., Dimou, L., Sutor, B., Berninger, B., and Götz, M. (2014). Sox2-mediated conversion of NG2 glia into induced neurons in the injured adult cerebral cortex. Stem Cell Reports *3*, 1000–1014.

Hollemann, T., Bellefroid, E., and Pieler, T. (1998). The Xenopus homologue of the Drosophila gene tailless has a function in early eye development. Development *125*, 2425–2432.

Islam, M.M., and Zhang, C.L. (2015). TLX: A master regulator for neural stem cell maintenance and neurogenesis. Biochim. Biophys. Acta *1849*, 210–216.

Kim, J.G., Armstrong, R.C., v Agoston, D., Robinsky, A., Wiese, C., Nagle, J., and Hudson, L.D. (1997). Myelin transcription factor 1 (Myt1) of the oligodendrocyte lineage, along with a closely related CCHC zinc finger, is expressed in developing neurons in the mammalian central nervous system. J. Neurosci. Res. *50*, 272–290.

Kitambi, S.S., and Hauptmann, G. (2007). The zebrafish orphan nuclear receptor genes nr2e1 and nr2e3 are expressed in developing eye and forebrain. Gene Expr. Patterns *7*, 521–528.

Koo, J.W., and Duman, R.S. (2008). IL-1beta is an essential mediator of the antineurogenic and anhedonic effects of stress. Proc. Natl. Acad. Sci. USA *105*, 751–756.

Li, W., Sun, G., Yang, S., Qu, Q., Nakashima, K., and Shi, Y. (2008). Nuclear receptor TLX regulates cell cycle progression in neural stem cells of the developing brain. Mol. Endocrinol. *22*, 56–64.

Liu, H.K., Belz, T., Bock, D., Takacs, A., Wu, H., Lichter, P., Chai, M., and Schütz, G. (2008). The nuclear receptor tailless is required for neurogenesis in the adult subventricular zone. Genes Dev. *22*, 2473–2478.

Lorthongpanich, C., Yang, S.H., Piotrowska-Nitsche, K., Parnpai, R., and Chan, A.W. (2008). Development of single mouse blastomeres into blastocysts, outgrowths and the establishment of embryonic stem cells. Reproduction *135*, 805–813.

Masui, S., Nakatake, Y., Toyooka, Y., Shimosato, D., Yagi, R., Takahashi, K., Okochi, H., Okuda, A., Matoba, R., Sharov, A.A., et al. (2007). Pluripotency governed by Sox2 via regulation of Oct3/4 expression in mouse embryonic stem cells. Nat. Cell Biol. *9*, 625–635.

Matsushita, F., Kameyama, T., Kadokawa, Y., and Marunouchi, T. (2014). Spatiotemporal expression pattern of Myt/NZF family zinc finger transcription factors during mouse nervous system development. Dev. Dyn. *243*, 588–600.

McKay, R. (1997). Stem cells in the central nervous system. Science *276*, 66–71.

Monaghan, A.P., Grau, E., Bock, D., and Schütz, G. (1995). The mouse homolog of the orphan nuclear receptor tailless is expressed in the developing forebrain. Development *121*, 839–853.

Monaghan, A.P., Bock, D., Gass, P., Schwäger, A., Wolfer, D.P., Lipp, H.P., and Schütz, G. (1997). Defective limbic system in mice lacking the tailless gene. Nature *390*, 515–517.

Niu, W., Zou, Y., Shen, C., and Zhang, C.L. (2011). Activation of postnatal neural stem cells requires nuclear receptor TLX. J. Neurosci. *31*, 13816–13828.

Niu, W., Zang, T., Zou, Y., Fang, S., Smith, D.K., Bachoo, R., and Zhang, C.L. (2013). In vivo reprogramming of astrocytes to neuroblasts in the adult brain. Nat. Cell Biol. *15*, 1164–1175.

Niu, W., Zang, T., Smith, D.K., Vue, T.Y., Zou, Y., Bachoo, R., Johnson, J.E., and Zhang, C.-L. (2015). SOX2 reprograms resident astrocytes into neural progenitors in the adult brain. Stem Cell Reports *4*, 780–794.

Pevny, L.H., and Nicolis, S.K. (2010). Sox2 roles in neural stem cells. Int. J. Biochem. Cell Biol. *42*, 421–424.

Rao, M.S. (1999). Multipotent and restricted precursors in the central nervous system. Anat. Rec. *257*, 137–148.

Rossant, J. (2004). Lineage development and polar asymmetries in the peri-implantation mouse blastocyst. Semin. Cell Dev. Biol. *15*, 573–581.

Roy, K., Kuznicki, K., Wu, Q., Sun, Z., Bock, D., Schutz, G., Vranich, N., and Monaghan, A.P. (2004). The Tlx gene regulates the timing of neurogenesis in the cortex. J. Neurosci. *24*, 8333–8345.

Sarkar, A., and Hochedlinger, K. (2013). The sox family of transcription factors: versatile regulators of stem and progenitor cell fate. Cell Stem Cell *12*, 15–30.

Shi, Y., Chichung Lie, D., Taupin, P., Nakashima, K., Ray, J., Yu, R.T., Gage, F.H., and Evans, R.M. (2004). Expression and function of orphan nuclear receptor TLX in adult neural stem cells. Nature *427*, 78–83.

Shi, Y., Sun, G., Zhao, C., and Stewart, R. (2008). Neural stem cell self-renewal. Crit. Rev. Oncol. Hematol. *65*, 43–53.

Shimozaki, K., Zhang, C.L., Suh, H., Denli, A.M., Evans, R.M., and Gage, F.H. (2012). SRY-box-containing gene 2 regulation of nuclear receptor tailless (Tlx) transcription in adult neural stem cells. J. Biol. Chem. *287*, 5969–5978.

Su, Z., Niu, W., Liu, M.L., Zou, Y., and Zhang, C.L. (2014). In vivo conversion of astrocytes to neurons in the injured adult spinal cord. Nat. Commun. *5*, 3338.

Suh, H., Consiglio, A., Ray, J., Sawai, T., D'Amour, K.A., and Gage, F.H. (2007). In vivo fate analysis reveals the multipotent and self-renewal capacities of Sox2+ neural stem cells in the adult hippocampus. Cell Stem Cell *1*, 515–528.

Sun, G., Yu, R.T., Evans, R.M., and Shi, Y. (2007). Orphan nuclear receptor TLX recruits histone deacetylases to repress transcription and regulate neural stem cell proliferation. Proc. Natl. Acad. Sci. USA *104*, 15282–15287.

Sun, G., Alzayady, K., Stewart, R., Ye, P., Yang, S., Li, W., and Shi, Y. (2010). Histone demethylase LSD1 regulates neural stem cell proliferation. Mol. Cell. Biol. *30*, 1997–2005.

Sun, G., Ye, P., Murai, K., Lang, M.F., Li, S., Zhang, H., Li, W., Fu, C., Yin, J., Wang, A., et al. (2011). miR-137 forms a regulatory loop with nuclear receptor TLX and LSD1 in neural stem cells. Nat. Commun. *2*, 529.

Wang, Y., Liu, H.K., and Schütz, G. (2013). Role of the nuclear receptor Tailless in adult neural stem cells. Mech. Dev. *130*, 388–390.

Weiss, S., and van der Kooy, D. (1998). CNS stem cells: where's the biology (a.k.a. beef)? J. Neurobiol. *36*, 307–314.

Yokoyama, A., Takezawa, S., Schüle, R., Kitagawa, H., and Kato, S. (2008). Transrepressive function of TLX requires the histone demethylase LSD1. Mol. Cell. Biol. *28*, 3995–4003.

Yu, R.T., McKeown, M., Evans, R.M., and Umesono, K. (1994). Relationship between Drosophila gap gene tailless and a vertebrate nuclear receptor Tlx. Nature *370*, 375–379.

Yu, R.T., Chiang, M.Y., Tanabe, T., Kobayashi, M., Yasuda, K., Evans, R.M., and Umesono, K. (2000). The orphan nuclear receptor Tlx regulates Pax2 and is essential for vision. Proc. Natl. Acad. Sci. USA *97*, 2621–2625.

Zhang, C.L., Zou, Y., Yu, R.T., Gage, F.H., and Evans, R.M. (2006). Nuclear receptor TLX prevents retinal dystrophy and recruits the corepressor atrophin1. Genes Dev. *20*, 1308–1320.

Zhang, C.L., Zou, Y., He, W., Gage, F.H., and Evans, R.M. (2008). A role for adult TLX-positive neural stem cells in learning and behaviour. Nature *451*, 1004–1007.

Zhao, C., Sun, G., Li, S., and Shi, Y. (2009). A feedback regulatory loop involving microRNA-9 and nuclear receptor TLX in neural stem cell fate determination. Nat. Struct. Mol. Biol. *16*, 365–371.

Zhao, C., Sun, G., Li, S., Lang, M.F., Yang, S., Li, W., and Shi, Y. (2010). MicroRNA let-7b regulates neural stem cell proliferation and differentiation by targeting nuclear receptor TLX signaling. Proc. Natl. Acad. Sci. USA *107*, 1876–1881.

Zhuo, L., Theis, M., Alvarez-Maya, I., Brenner, M., Willecke, K., and Messing, A. (2001). hGFAP-cre transgenic mice for manipulation of glial and neuronal function in vivo. Genesis *31*, 85–94.